

# Evaluation of microvascular density in Barrett's associated neoplasia

Vani JA Konda<sup>1</sup>, John Hart<sup>2</sup>, Shang Lin<sup>3</sup>, Maria Tretiakova<sup>2</sup>, Ilyssa O Gordon<sup>2</sup>, Lucas Campbell<sup>2</sup>, Anirudh Kulkarni<sup>4</sup>, Marc Bissonnette<sup>4</sup>, Stefan Seewald<sup>5</sup> and Irving Waxman<sup>1</sup>

<sup>1</sup>Center for Endoscopic Research and Therapeutics, Section of Gastroenterology, University of Chicago Medical Center, Chicago, IL, USA; <sup>2</sup>Department of Pathology, University of Chicago Medical Center, Chicago, IL, USA; <sup>3</sup>Department of Health Studies, University of Chicago Medical Center, Chicago, IL, USA; <sup>4</sup>Department of Gastroenterology, University of Chicago Medical Center, Chicago, IL, USA and <sup>5</sup>Section of Gastroenterology, Klinik Hirslanden, Zurich, Switzerland

**Angiogenesis has an important role in the carcinogenesis of esophageal adenocarcinoma, however, the diagnostic and prognostic utility of microvascular density counts have not been clinically established. The aim of this study is to assess the correlation between microvascular density and disease progression of non-dysplastic Barrett's esophagus, low-grade dysplasia, high-grade dysplasia and invasive carcinoma in the superficial aspects of the tissue. Archival histological specimens from two referral centers for Barrett's esophagus and esophageal cancer were selected for review. A total of 160 regions marked according to histological grade were assessed with digitally interactive software to measure microvascular density. This was quantified in three levels: 0–50, 50–100 and 100–150  $\mu\text{m}$ . In the areas of gastric cardia, Barrett's esophagus, low-grade dysplasia, high-grade dysplasia and cancer, microvascular density was significantly different ( $P < 0.0001$ ) among the five groups in the most superficial 150  $\mu\text{m}$  of the mucosa. Furthermore, when examining the pairwise difference between the groups, there was a significant difference between cancer and each of the lower grades of histology ( $P < 0.05$ ) and between high-grade dysplasia and each of the lower grades of histology ( $P < 0.05$ ). These statistically significant differences were preserved in examining the depth at the most superficial 50  $\mu\text{m}$ . We have used digital pathology to demonstrate a significant and stepwise increase in microvascular density, which supports the hypothesis that angiogenesis has a key role in Barrett's carcinogenesis. Furthermore, the differences in the most superficial mucosal layers are consistent with findings of increased vascularity by depth-restricted imaging modalities.**

*Modern Pathology* (2013) **26**, 125–130; doi:10.1038/modpathol.2012.146; published online 24 August 2012

**Keywords:** angiogenesis; Barrett's esophagus; esophageal cancer; microvascular density

Angiogenesis has an important role in the carcinogenesis of esophageal adenocarcinoma, however, the diagnostic and prognostic utility of microvascular density counts have not been clinically established.<sup>1,2</sup> Esophageal adenocarcinoma arises from Barrett's esophagus in a metaplasia–dysplasia–carcinoma sequence. Intestinal metaplasia and dysplasia have been studied in terms of microvascular density, and neoangiogenesis is thought to begin in these precursor lesions.<sup>3–7</sup>

Endoscopists are exploiting neovascularization in Barrett's esophagus to detect neoplasia using novel imaging modalities, such as narrow band imaging and confocal laser endomicroscopy.<sup>8–12</sup> One of the features that endoscopists look for is the vascular pattern under narrow band imaging or confocal laser endomicroscopy.<sup>8–12</sup> Irregular or increased vascularity is a feature that endoscopists are looking for with these imaging modalities to identify significant superficial neoplasia, including both high-grade dysplasia and esophageal adenocarcinoma.

The aim of this study is to assess the correlation between microvascular density and disease progression of non-dysplastic Barrett's esophagus, low-grade dysplasia, high-grade dysplasia and invasive carcinoma in the superficial aspects of the tissue.

Correspondence: Dr VJA Konda, Center for Endoscopic Research and Therapeutics, Section of Gastroenterology, University of Chicago Medical Center, 5841S. Maryland Avenue MC 4076, Chicago, IL 60637, USA.

E-mail: vkonda@medicine.bsd.uchicago.edu

Received 24 April 2012; revised 15 July 2012; accepted 16 July 2012; published online 24 August 2012

## Materials and methods

### Tissue Selection and Immunohistochemical Staining

Following a protocol approved by the Institutional Review Board, archived H&E-stained slides from 75 endoscopic and surgical resection specimens with Barrett's associated neoplasia from two centers were reviewed. Forty cases of patients with Barrett's associated neoplasia were selected for study. From review of H&E slides, 160 areas were selected. Areas of BE, low-grade dysplasia, high-grade dysplasia and invasive cancer were marked for further analysis. This was performed by two investigators, one of whom is an experienced gastrointestinal pathologist (JH). Corresponding formalin-fixed and paraffin-embedded tissue blocks were sectioned and stained with anti-CD31 antibody (Dako, Carpinteria, CA, USA).

In brief, 4- $\mu\text{m}$  sections were deparaffinized in xylenes, rehydrated through graded ethanol solutions to distilled water and then washed in Tris-buffered saline. CD31 antigen was retrieved using high-temperature treatment in citrate buffer for 15 min in a microwave oven. Endogenous peroxidase activity was quenched by incubation in 3%  $\text{H}_2\text{O}_2$  in methanol for 5 min. Nonspecific binding sites were blocked using Protein Block (Dako) for 20 min. Then tissue sections were incubated for 1 h at room temperature with the mouse monoclonal antibodies against CD31 (clone JC70A, 1:40; Dako). This step was followed by 30 min incubation with goat anti-mouse IgG conjugated to a horse-radish peroxidase-labeled polymer (Envision<sup>TM</sup>+ System; Dako).

Areas of obvious inflammation with lymphocytic infiltrate were excluded from further analysis. Areas were selected for analysis based on the preidentified marked areas. In cases where the corresponding immunostained section appeared to not represent the H&E section, these cases were reviewed by two investigators, including an experienced gastrointestinal pathologist (JH), and excluded or reclassified as appropriate. Microvascular density was quantified in histological fields representative of gastric cardia, non-dysplastic Barrett' esophagus, low-grade dysplasia, high-grade dysplasia and cancer.

From forty cases of patients with Barrett's esophagus who underwent therapy for associated neoplasia, 160 areas were selected from review of H&E slides and areas marked for analysis (Figure 1). The histological grades of the selected areas are shown in Table 1. Also, 154 areas were examined at 50  $\mu\text{m}$  increments of the 150 most superficial aspect of the tissue in that area.

### Microvascular Density Analysis

The Automated Cellular Imaging System (ACIS) from Clariant (San Juan Capistrano, CA, USA) was used to quantify microvascular density as described

previously.<sup>13</sup> The ACIS consists of an Olympus bright field microscope with five objectives (UPFL  $\times 4$ ,  $\times 10$ ,  $\times 20$ ,  $\times 40$  and  $\times 60$ ), digital camera (CCD, Sony), an automated slide loading system for 100 slides and a PC. The ACIS technology automatically loads conventional IHC microscope slides for scanning at high resolution. Each high-resolution image is then imported into the application software and is available for analysis. The image analysis system's microvascular density application was configured for vessel detection based on applying chromogen masks for high chromogenic staining (brown threshold) and counterstaining (blue threshold), and the minimal and maximal size of the vessels. After selection of appropriate regions for microvascular density counting, the following measurements were captured digitally for each selected region of tissue: total vessel count, mean vessel area (square microns occupied by positively stained vessels) and microvascular density, or vessel to tissue area ratio (vessel density percentage calculated by area of blood vessels occupying area of counterstained tissue). Then, microvascular density was quantified in 50  $\mu\text{m}$  diameter areas in three levels: 0–50, 50–100 and 100–150  $\mu\text{m}$ .

### Statistical Analysis

ANOVA and Kruskal–Wallis nonparametric tests were used to examine whether there were differences in microvascular density among the tissue of five areas: cardia, Barrett's, low-grade dysplasia, high-grade dysplasia and invasive cancer. If such differences existed, then Tukey's studentized range test was used to identify where the differences were and to compare their magnitudes.

## Results

In examining the microvascular density in the most superficial 150  $\mu\text{m}$  of the tissue in the areas of gastric cardia, Barrett' esophagus, low-grade dysplasia, high-grade dysplasia and cancer, there was a statistically significant difference of  $P < 0.0001$  among the five groups. Furthermore, when examining the pairwise difference between the groups, there was a statistically significant difference between cancer and each of the lower grades of histology, as well as between high-grade dysplasia and each of the lower grades of histology ( $P < 0.05$ ) (Figures 2 and 3).

In examining the depth at the most superficial 50  $\mu\text{m}$ , there was also a statistically significant difference among the five groups ( $P < 0.0001$ ) as seen in Figure 3. Pairwise comparison also indicated that statistically significant difference between cancer and each of the lower grades of histology and between high-grade dysplasia and each of the lower grades of histology was preserved ( $P < 0.05$ ). At a slightly lower depth of 50–100  $\mu\text{m}$  below the surface,

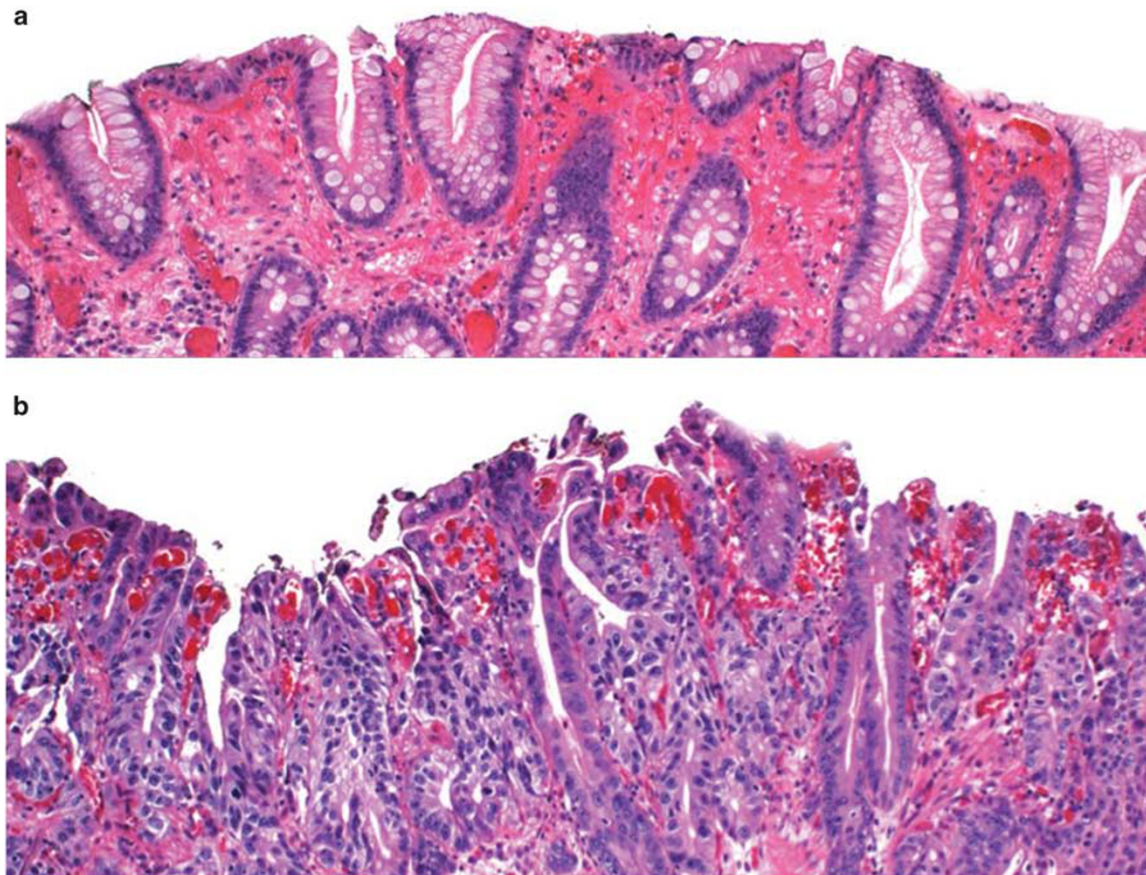


**Figure 1** H&E staining of non-dysplastic Barrett's esophagus (a) and Barrett's esophagus with HGD (b).

**Table 1** Histology of areas marked for analysis

<i>Histology</i>	<i>Number</i>
Gastric	13
Non-dysplastic Barrett's esophagus	33
Barrett's esophagus with low-grade dysplasia	34
Barrett's esophagus with high-grade dysplasia	68
Esophageal adenocarcinoma	12

there was a statistically significant difference among the five groups ( $P < 0.0001$  using ANOVA and Kruskal–Wallis nonparametric tests), and cancer remained to have a statistically significant difference from each of the lower grades of histology ( $P < 0.05$  using Tukey's studentized range test). However, only high-grade dysplasia was statistically significantly different between non-dysplastic Barrett' esophagus and gastric cardia at this depth ( $P < 0.05$  using Tukey's studentized range test). At even a lower depth of 100–150  $\mu\text{m}$  below the surface, there remained a statistically significant difference among the groups ( $P < 0.001$  ANOVA and Kruskal–Wallis nonparametric tests), but the between pairwise group differences were preserved only for the cancer group when compared with non-dysplastic Barrett's and stomach, respectively.

## Discussion

We utilized digital pathology techniques to assess the correlation between microvascular density and disease progression of non-dysplastic BE, low-grade dysplasia, high-grade dysplasia and cancer in the superficial aspects of the tissue. We found a significant stepwise increase in microvascular density from normal gastric cardia to non-dysplastic Barrett' esophagus, to low-grade dysplasia, to high-grade dysplasia and finally to cancer.

This increase in microvascular density supports the hypothesis that angiogenesis has a key role in the metaplasia–carcinoma progression and supports findings in previous studies.<sup>1–6,14,15</sup> Although previous studies established a trend in the metaplasia–dysplasia–carcinoma sequence, none have clearly demonstrated whether high-grade dysplasia is significantly different from metaplasia or low-grade dysplasia. Our study specifically demonstrates a significant and stepwise increase in microvascular density between Barrett' esophagus, low-grade dysplasia and high-grade dysplasia, which has not been previously shown. This finding is clinically relevant because endoscopists often use tools relying on vascularity for detection and targeting of areas of high-grade dysplasia and cancer. It is clinically useful to distinguish these different pathologies at

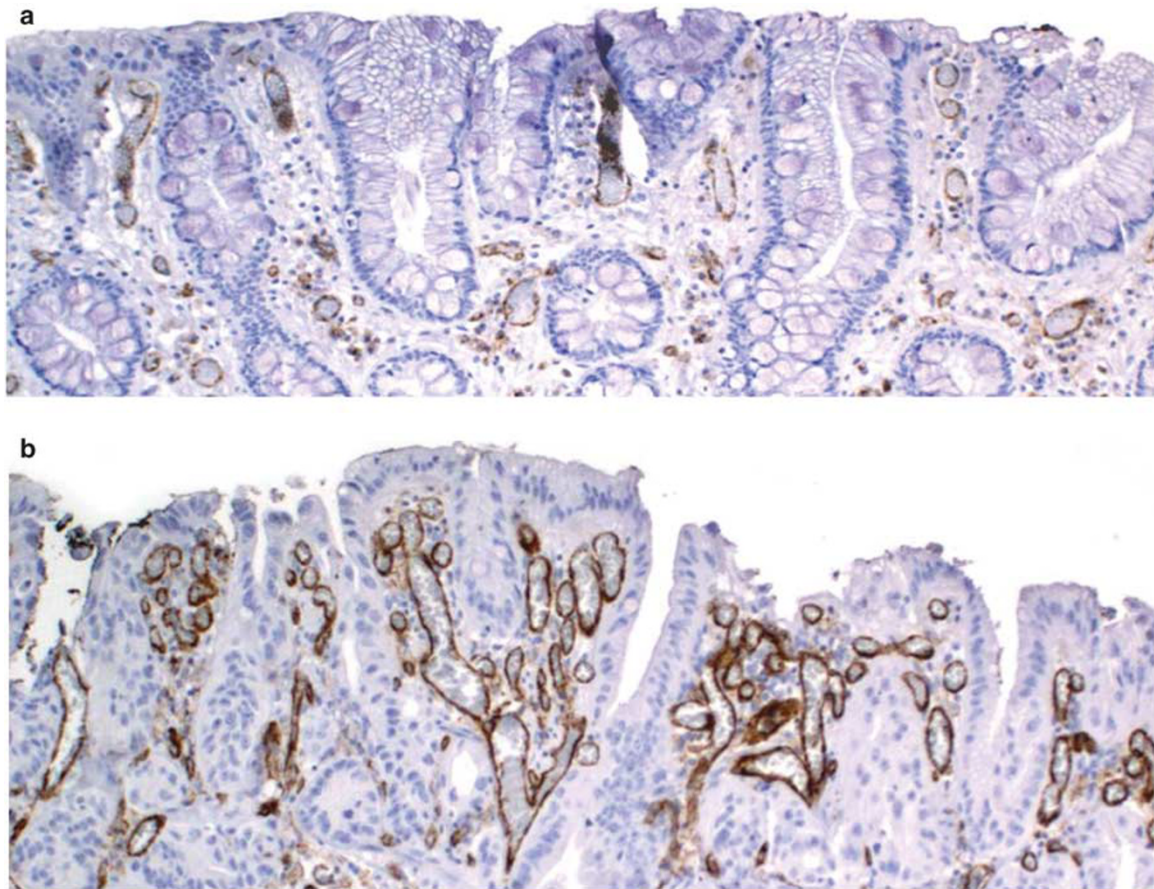


**Figure 2** Immunohistochemistry with staining of CD31 of tissue with non-dysplastic Barrett's esophagus (a) and Barrett's esophagus with HGD (b). Note the relative increase in staining in the dysplastic epithelium.

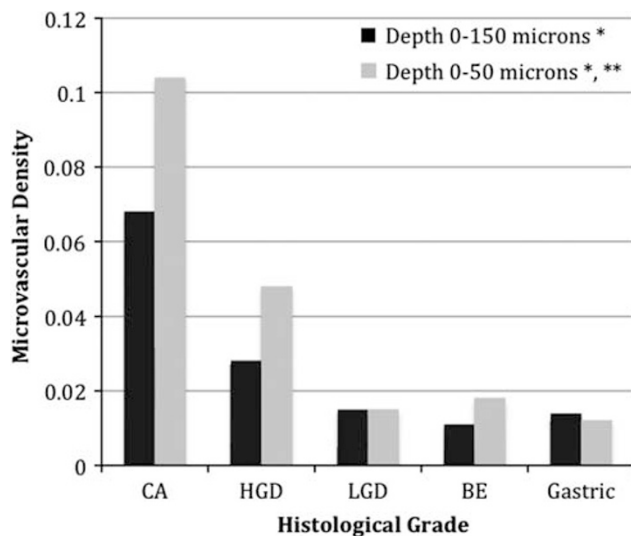


**Figure 3** Microvascular density by histology in Barrett's neoplasia at superficial depths. The trend was statistically significant among the five groups ( $P < 0.0001$ ). Also, pairwise comparisons of CA with each of the lower grades of histology and of HGD with each of the lower grades of histology yielded  $P$ -values of  $< 0.05$  when considering multiple comparisons. \*\*Depths of 50–100 microns and 100–150 microns were also examined. The most superficial depths of 0–50 microns demonstrated the most difference in MVD. BE, non-dysplastic Barrett's esophagus; CA, invasive cancer; HGD, high-grade dysplasia; LGD, low-grade dysplasia.

endoscopy, because high-grade dysplasia warrants intervention, whereas low-grade dysplasia and non-dysplastic Barrett's esophagus may be managed with surveillance.

Furthermore, some endoscopic imaging technologies are restricted by depth. Previous studies are based on surgical specimens or biopsy material without details as to the depth of the analyzed areas.<sup>3,4,6</sup> This study systematically approached the analysis of specimens in relation to the depth from the surface. Not only do cancer and high-grade dysplasia have statistically significant differences from each of the lower grades of histology in the superficial aspects (150  $\mu\text{m}$ ) of the tissue, but these differences persist in even the most superficial 50  $\mu\text{m}$  of the tissue.

This is clinically relevant with some of the increasingly popular imaging technologies for Barrett's esophagus. For example, narrow band imaging illuminates the tissue with filtered blue light (peaking at 415 nm) and green light (540 nm).<sup>16</sup> These bands are strongly absorbed by hemoglobin, enabling visualization of the superficial capillary network and submucosal vessels (Figure 4). The blue light has an average penetration depth of around 170  $\mu\text{m}$ . The visualization of this superficial capillary network would detect the stepwise increase in microvascular

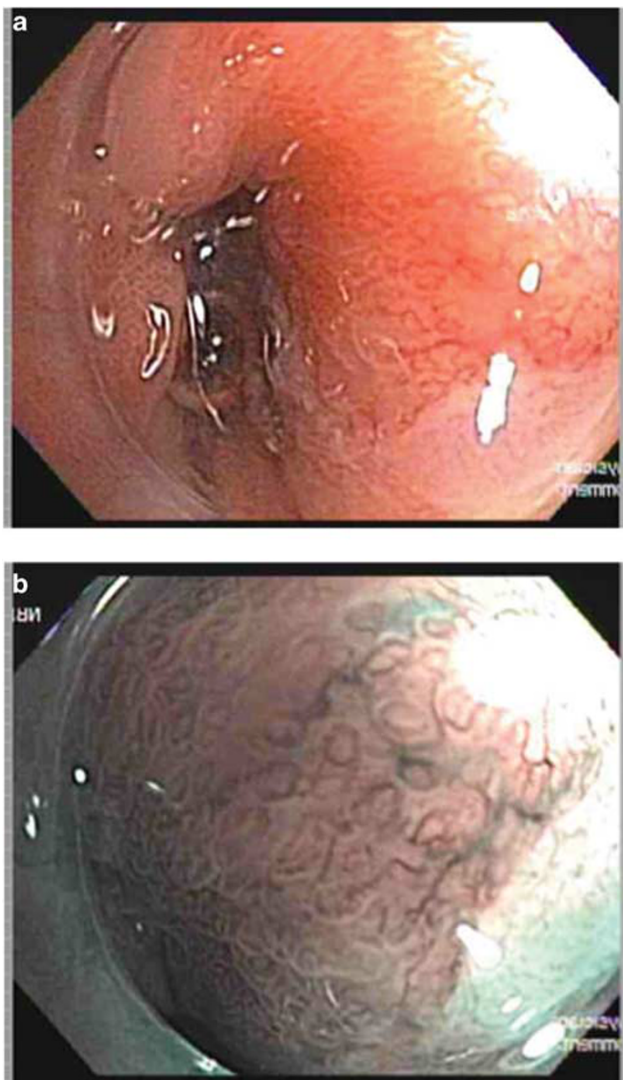


**Figure 4** An area of Barrett's esophagus with vascularity noted by white light endoscopy (a) and NBI (b).

density that this study demonstrates in the most superficial  $150\ \mu\text{m}$  of the tissue. Another novel imaging technology is confocal laser endomicroscopy<sup>17</sup> (Figure 5). The endomicroscope (Pentax, Montvale, NJ, USA; Optiscan, Victoria, Australia) has variable depth imaging ranging  $0\text{--}250\ \mu\text{m}$ . The probe-based confocal system (Mauna Kea Technologies, Paris, France) has a fixed penetration depth of  $55\text{--}65\ \mu\text{m}$  with the ultra high-definition probe. Again, the superficial differences as suggested by the total superficial  $150\ \mu\text{m}$  depth and, specifically, the most superficial  $50\ \mu\text{m}$  depth in our study suggest that these are appropriate ways to target vascularity.

Irregular vascularity visualized by narrow band imaging or confocal laser endomicroscopy has been identified as a maker for neoplasia.<sup>11,12,18</sup> Currently, imaging is largely a subjectively based process. However, further development of image software may provide means to quantify *in vivo* imaging. Becker *et al.*<sup>8</sup> used a prototype software to determine

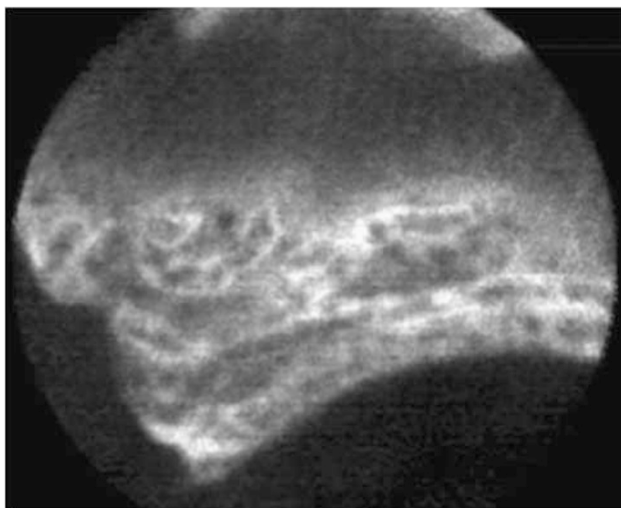


**Figure 5** Confocal laser endomicroscopy demonstrating increased vascularity. Note the erythrocytes coursing through the vessels.

differences in microvascular area as assessed by confocal endomicroscopy in Barrett's esophagus. Some challenges of quantification by such software include the extravasation of fluorescein from the blood vessels and the more leaky blood vessels seen in neoplasia. Additionally, inflammation presents a challenge as a possible confounding factor. Future directions may look at further ways to detect or quantify vascularity to help differentiate grades of dysplasia in real time to target biopsies and resections in Barrett's esophagus.

In conclusion, we have used digital pathology to demonstrate a significant and stepwise increase in microvascular density, which supports the hypothesis that angiogenesis has a key role in the metaplasia–dysplasia–carcinoma progression in Barrett's esophagus. Furthermore, the differences in the most superficial mucosal layers are consistent with findings relevant to vascularity by depth-restricted imaging modalities.

## Acknowledgements

This study was supported by the Gastrointestinal Research Fund's Associate Board Pilot Award. Drs Konda, Waxman and Hart have received honoraria from Mauna Kea Technologies.

## Disclosure/conflict of interest

The authors declare no conflict of interest.

## References

- 1 Lord RV, Park JM, Wickramasinghe K, *et al*. Vascular endothelial growth factor and basic fibroblast growth factor expression in esophageal adenocarcinoma and Barrett esophagus. *J Thorac Cardiovasc Surg* 2003;125: 246–253.

- 2 Torres C, Wang H, Turner J, *et al*. Prognostic significance and effect of chemoradiotherapy on microvessel density (angiogenesis) in esophageal Barrett's esophagus-associated adenocarcinoma and squamous cell carcinoma. *Hum Pathol* 1999;30:753–758.
- 3 Auvinen MI, Sihvo EI, Ruohtula T, *et al*. Incipient angiogenesis in Barrett's epithelium and lymphangiogenesis in Barrett's adenocarcinoma. *J Clin Oncol* 2002;20:2971–2979.
- 4 Mobius C, Stein HJ, Becker I, *et al*. Vascular endothelial growth factor expression and neovascularization in Barrett's carcinoma. *World J Surg* 2004;28:675–679.
- 5 Mobius C, Stein HJ, Becker I, *et al*. The 'angiogenic switch' in the progression from Barrett's metaplasia to esophageal adenocarcinoma. *Eur J Surg Oncol* 2003;29:890–894.
- 6 Couvelard A, Paraf F, Gratio V, *et al*. Angiogenesis in the neoplastic sequence of Barrett's oesophagus. Correlation with VEGF expression. *J Pathol* 2000;192:14–18.
- 7 Moriyama N, Amano Y, Mishima Y, *et al*. What is the clinical significance of stromal angiogenesis in Barrett's esophagus? *J Gastroenterol Hepatol* 2008;23 (Suppl 2):S210–S215.
- 8 Becker V, Vieth M, Bajbouj M, *et al*. Confocal laser scanning fluorescence microscopy for *in vivo* determination of microvessel density in Barrett's esophagus. *Endoscopy* 2008;40:888–891.
- 9 Pohl H, Rosch T, Vieth M, *et al*. Miniprobe confocal laser microscopy for the detection of invisible neoplasia in patients with Barrett's oesophagus. *Gut* 2008;57:1648–1653.
- 10 Kiesslich R, Gossner L, Goetz M, *et al*. *In vivo* histology of Barrett's esophagus and associated neoplasia by confocal laser endomicroscopy. *Clin Gastroenterol Hepatol* 2006;4:979–987.
- 11 Sharma P, Meining AR, Coron E, *et al*. Real-time increased detection of neoplastic tissue in Barrett's esophagus with probe-based confocal laser endomicroscopy: final results of an international multicenter, prospective, randomized, controlled trial. *Gastrointest Endosc* 2011;74:465–472.
- 12 Sharma P, Bansal A, Mathur S, *et al*. The utility of a novel narrow band imaging endoscopy system in patients with Barrett's esophagus. *Gastrointest Endosc* 2006;64:167–175.
- 13 Westerhoff M, Tretiakova M, Hovan L, *et al*. CD61, CD31, and CD34 improve diagnostic accuracy in gastric antral vascular ectasia and portal hypertensive gastropathy: an immunohistochemical and digital morphometric study. *Am J Surg Pathol* 2010;34:494–501.
- 14 Mobius C, Stein HJ, Spiess C, *et al*. COX2 expression, angiogenesis, proliferation and survival in Barrett's cancer. *Eur J Surg Oncol* 2005;31:755–759.
- 15 Zampeli E, Karamanolis G, Morfopoulos G, *et al*. Increased expression of VEGF, COX-2, and Ki-67 in Barrett's esophagus: does the length matter? *Dig Dis Sci* 2012;57:1190–1196.
- 16 Waxman I, Konda VJ. Endoscopic techniques for recognizing neoplasia in Barrett's esophagus: which should the clinician use? *Curr Opin Gastroenterol* 2010;26:352–360.
- 17 Goetz M, Watson A, Kiesslich R. Confocal laser endomicroscopy in gastrointestinal diseases. *J Biophotonics* 2011;4:498–508.
- 18 Wallace M, Lauwers GY, Chen Y, *et al*. Miami classification for probe-based confocal laser endomicroscopy. *Endoscopy* 2011;43:882–891.